

# Manufacturing Free-Standing Graphene Oxide/Carbon Nanotube Hybrid Papers and Improving Electrical Conductivity by a Mild Annealing Treatment

R.A. Oliveira<sup>a,b,\*</sup> , J.P. Nascimento<sup>a,b</sup> , M. H. A. Zanin<sup>c</sup> , L. F. P. Santos<sup>a,b</sup> , B. Ribeiro<sup>a,d</sup> ,  
A. Guimarães<sup>a</sup> , E. C. Botelho<sup>b</sup> , M. L. Costa<sup>a,b</sup> 

<sup>a</sup>Instituto de Pesquisas Tecnológicas (IPT), Departamento de Materiais Avançados, Laboratório de Estruturas Leves (LEL), São José dos Campos, SP, Brasil.

<sup>b</sup>Universidade Estadual Paulista (UNESP), Faculdade de Engenharia e Ciências de Guaratinguetá, Departamento de Materiais e Tecnologia, Guaratinguetá, SP, Brasil.

<sup>c</sup>Instituto de Pesquisas Tecnológicas (IPT), Laboratório de Processos Químicos e Tecnologia de Partículas (LPP), São Paulo, SP, Brasil.

<sup>d</sup>Universidade Federal De São Paulo (UNIFESP), Laboratório de Tecnologia de Polímeros e Biopolímeros (TecPBio), São José dos Campos, SP, Brasil.

Received: March 17, 2022; Revised: September 30, 2022; Accepted: October 04, 2022

The present work aims to evaluate the manufacturing processes of free-standing graphene oxide (GO)/reduced graphene oxide(rGO)/carbon nanotube (MWCNT) papers-like and the effect on electrical conductivities after annealing treatment. The pure GO and the hybrid papers were obtained by vacuum filtration and submitted to mild thermal annealing at 400 °C under an argon atmosphere. Analyses comparing the carbon paper-like materials before and after thermal treatment were done by thermogravimetric analysis (TGA), Raman spectroscopy, scanning electron microscopy (SEM), and electrical conductivity measurements. The characterization results show the annealing process effect on the morphology of paper materials. The GO papers and the hybrid (GO/rGO/MWCNT) exhibited good free-standing structure properties. The SEM results suggest the formation of gas void due to the thermal treatment. TGA and Raman results showed the thermal reduction and restoration of the carbon sp<sup>2</sup> network of the graphene oxide induced by thermal treatment. The thermal treatment was responsible for changing the almost insulator characteristic of free-standing pure GO paper, achieving an electrical conductivity of 752 S/m, and improving 45% of the free-standing hybrid carbon nanomaterials papers (GO/rGO/MWCNT) electrical conductivity, achieving the value of 1020 S/m.

**Keywords:** *graphene oxide, multi-walled carbon nanotubes, carbon nanomaterials, electrical conductivity, graphene paper.*

## 1. Introduction

In the last two decades, we have seen a considerable expansion of knowledge in different fields of graphene research and development. The graphene interest became higher after 2004 when K. Novoselov and A. Geim obtained the 2D carbon structure by micro-mechanical exfoliation, the scotch tape method, experimentally proving the excellent electronic properties expected by theory physic studies<sup>1</sup> and receiving six years later the Physic Nobel Prize. Since this event, the academy and the industry have invested a solid effort to achieve a higher technology readiness level (TRL) for many graphene applications<sup>2,3</sup>. Searching at the SCOPUS (Elsevier) base by the term graphene, this topic has achieved the mark of twenty-four thousand and four hundred related documents published yearly, demonstrating how interesting the subject is. The results of this engagement are turning possible concepts suggested by the vanguard at the beginning of the graphene revolution<sup>4</sup>. For example, it is possible to consider enhanced composite materials<sup>5-7</sup> development, electronic

devices<sup>8</sup> and sensors<sup>9,10</sup>, medical biosensors<sup>11</sup>, filtration membranes<sup>12,13</sup>, solutions applied for energy generation<sup>14</sup> and energy storage systems (ESS) applications<sup>15-18</sup> such as batteries and supercapacitors.

In the ESS field, graphene and its derivatives are the most studied active material in the design of supercapacitor electrodes related to the high theoretical surface area (2630 m<sup>2</sup>g<sup>-1</sup>) associated with 2D ion transport channels, good electrical conductivity as properly exfoliated (≤ 10 layers), excellent interfacial integrity and inter-layer spacing even after re-stacking. The intrinsic and specific capacitance of graphene, respectively, 21 μFcm<sup>-2</sup> and above 550 Fg<sup>-1</sup>, are higher than values observed in the literature for activated charcoal<sup>19,20</sup> or glassy-like carbon artifacts<sup>21,22</sup>. These properties of graphene are beneficial in increasing the performance of supercapacitors. Between the different manufacturing methods of graphene application in this field, the production of free-standing carbon nanomaterials paper-like by vacuum filtration is interesting because it is simple, clean, with low cost, and without involving the conducting additives and binders<sup>23</sup>.

\*e-mail: [rodrigo.a.oliveira@unesp.br](mailto:rodrigo.a.oliveira@unesp.br)

Another attractive characteristic of this manufacturing process for electrode design is the possibility of developing hybrid structures (such as graphene oxide and carbon nanotubes), and it is known that the combination of two nanomaterials can have a synergistic effect on essential properties which can improve the performance of the supercapacitor<sup>24-26</sup>.

In this work, the free-standing papers-like of pure graphene oxide (GO) and hybrid concepts consisting of mixtures of graphene oxide, reduced graphene oxide (rGO), and carbon nanotube (MWCNT) were produced from commercial constituents. Besides, regarding previous studies<sup>27</sup>, the effect of a mild thermal annealing treatment was evaluated on the papers-like by different characterization techniques.

## 2. Materials and Experimental Methods

### 2.1. Materials

The graphene oxide (GO), the reduced graphene oxide (rGO), and the functionalized multi-walled carbon nanotubes (MWCNT) were supplied by the company Nanografi. According to the supplier, the GO was produced by chemical exfoliation by a modified Hummers method, and the purification was done by washing with chemicals reagents and distilled water. The GO reduction process to obtain the rGO was performed by a chemical process. The GO and rGO datasheets inform a surface area (SA) of 420 m<sup>2</sup>/g and 1562 m<sup>2</sup>/g, respectively, number of layers  $\leq 5$  and purity degree of 99.5% for both materials and lateral length reported for GO is 7.5  $\mu\text{m}$  and for rGO is between 1 and 5  $\mu\text{m}$ . The MWCNT was produced by the CVD technique using Argon gas at 700 °C - 1200 °C. The supplier datasheet indicates that the MWCNT has 0.3 wt% of carboxyl groups (COOH), outside diameter between 48-78 nm, inside diameter between 5-10 nm, the length between 10-30  $\mu\text{m}$ , SA of 25 m<sup>2</sup>/g and 99.9% of purity degree. The GO was received with the appearance of slices of the film, demanding a thin razor lamina to cut it into small pieces to improve the dispersion performance during the sonication process. Whereas the rGO and MWCNT delivered have a powder aspect, the materials were applied as received. Additional information about the carbon nanomaterials acquired in this work is available on the supplier website<sup>28</sup> by tracking the commercial codes GO (NG01GO0102), rGO (NG01RGO0101) and MWCNT (NG01GM0115). Isopropyl alcohol 99.5% (CAS: 67-63-0) was used as a liquid medium for the preparation of dispersions.

### 2.2. Experimental methods

The manufacturing processes of the free-standing carbon nanomaterials papers were based on previous methods reported in the literature<sup>29-32</sup>. First, the GO solution was prepared by adding 60 mg of carbon nanomaterial to 100 mL of isopropyl alcohol to obtain the GO paper-like. To define the free-standing hybrid paper, a preliminary study was carried out considering the weight dispersion ratios of GO, rGO, and MWCNT demonstrated in Table 1. This optimization stage was essential to support the definition of the final hybrid graphene oxide paper, evaluating the manufacturability, the microscopy morphologies, and the electrical conductivity of the configuration of initial papers, and so, defining the ratios of the constituents for the final free-standing hybrid paper.

The solutions were immersed into an ice bath and dispersed with an ultrasonicator (Hielscher model UP400St) for 60 min (Figure 1) in a power configuration mode set at 70% and the cycle frequency at 50%. Afterward, the carbon nanomaterials papers were obtained by vacuum filtration system (Figure 1) on a nylon membrane filter (47 mm in diameter, 0.45  $\mu\text{m}$  pore size). The nylon membranes with the stacked carbon nanomaterials were carefully laid between two glass Petri plates and dried at 100 °C for 60 min. Finally, the carbon nanomaterials papers were peeled from the membrane filter. The pure GO and hybrid free-standing papers produced were subjected to a mild thermal annealing process, starting with a temperature ramp of 10 °C/min up to 400 °C, followed by 30 minutes of dwell under an argon flow of 15 L/min in a muffle furnace with 10 L of capacity. The paper thicknesses were estimated by the mean of ten measurements evaluating a slice of sample cross-section vertically positioned in an Opto-digital microscope (DSX500 – OLYMPUS) with a 5x order of magnitude from an optical lens, and 4x of digital zoom in a dark field mode.

The free-standing carbon nanomaterials papers were characterized by thermogravimetric analysis (TGA), Raman spectroscopy, scanning electron microscopy (SEM) and electrical conductivity measurements. The TGA were performed in a TA instrument Q500 equipment. The samples, with a mass of 5 mg, were heated in an alumina crucible from room temperature to 400 °C at 10 °C/min under a nitrogen flow of 50 mL/min. The Raman scattering spectra were measured in a Raman Witec Alpha 500 in the range of 1000 cm<sup>-1</sup> to 3500 cm<sup>-1</sup> using a 532 nm (2.33 eV) laser at approximately 1 mW, 600 line/mm diffraction grid and 100x objective. The SEM samples were examined by a scanning electronic

**Table 1.** Carbon materials mass concentrations applied at paper-like manufacturing samples.

Sample ID.	GO	rGO	MWCNT
	weight (mg) - [wt%]		
GO	60 [100%]	-	-
rGO_52%	43 [48.3%]	46 [51.7%]	-
rGO_67%**	23 [32.9%]	47 [67.1%]	-
rGO_76% **	18 [23.7%]	58 [76.3%]	-
rGO**	-	[100%]	-
MWCNT_16%*	51 [83.6%]	-	10 [16.4%]

\* Sample pulled out from the filter membrane presenting a brittle aspect. \*\* Samples that did not stacked from the filter membrane.

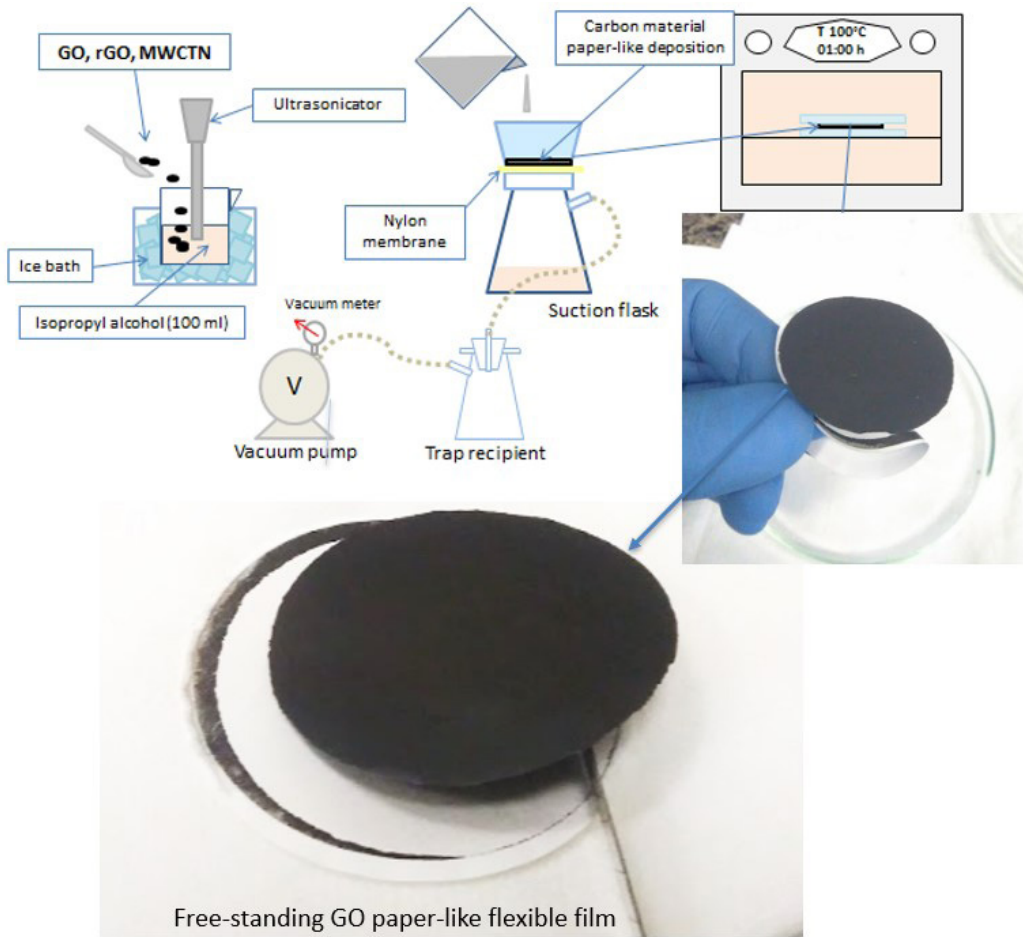


**Figure 1.** Summarized carbon nanomaterials papers manufacturing processes.

microscope ZEISS, model EVO-MA10 with accelerating voltage of 20 kV. Prior to SEM analysis, specimens were coated with gold-palladium using a mini Sputter Coater model POLARON EMITECH SC7620 to improve a conductive surface in a high vacuum atmosphere. The sputtering coating was done using a tension approximately of 800 V, and the process duration was of 120 seconds with a nominal velocity of 3 Å/s. The sheet resistance of the papers was analyzed at a four-point test fixture, with gold contact wires being the externals adjusted with 5 mm of distance and the others equidistant disposed, at a JANDEL electronic station, model RM3000. The electrical conductivity was calculated according to Equation 1, regarding Ribeiro et al<sup>29</sup>:

$$\sigma_{DC} = (R_s \cdot t)^{-1} \quad (1)$$

Where  $\sigma_{DC}$  represents the electrical film conductivity in a continuous current, the  $R_s$  is the sheet resistance ( $\Omega/\square$ ), and  $t$  represents the thickness ( $m$ ) of the carbon paper-like.

### 3. Results and Discussions

The first stage of the processability evaluation shows the dependency of the paper stability according to the GO

ratio considered at the dispersion (see remarks in Table 1). The free-standing pure GO paper presents a simple pull-out operation from the filter and flexible structure characteristic, with 0.043 mm of thickness. Despite the brittle aspect of the rGO\_52% and MWCNT\_16% papers, it was possible to proceed with the filter pull-out operation and measure the thickness film, presenting 0.17 mm and 0.14 mm, respectively. The electrical conductivity papers confirm the insulating property of the GO paper, as expected. The rGO\_52% and MWCNT\_16% papers show negligible conductivities, 5 S/m and 75 S/m, respectively. The SEM evaluation of these samples suggests that the low conductivity results are related to a poor connection between the rGOs anchored at the GO structure, depicted in Figure 2, and the discontinuity of the MWCNT mat, presented in Figure 3.

After these analyses, the manufacturing papers procedures were improved, maintaining the free-standing pure GO paper and producing the hybrid paper production with constituents' ratio of 50 wt% GO, 25 wt% rGO, and 25 wt% MWCNT, aiming to improve the MWCNT mat connectivity and, consequently, the electrical conductivity of the paper also considering the properties of rGO included. Although less flexible than the GO paper sample, this new hybrid paper

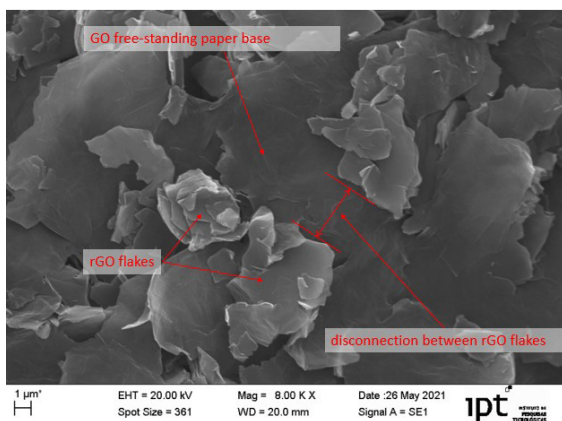


**Figure 2.** SEM image: the disconnected rGO flakes decorating GO paper at the rGO\_52% sample.

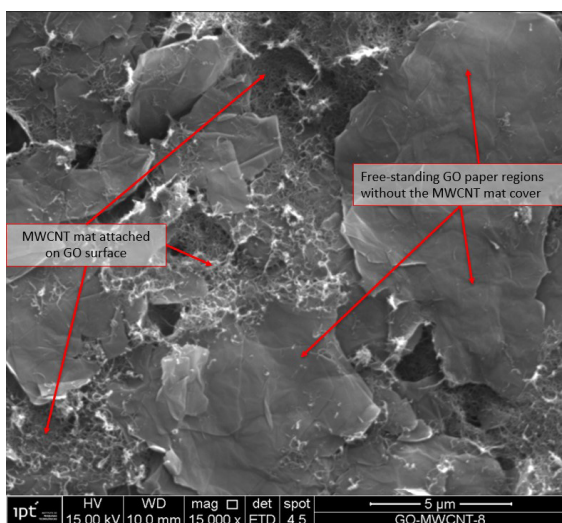


**Figure 3.** SEM image: the discontinuity of MWCNT mat at the GO paper surface at MWCNT\_16% sample.

configuration presented a good filter pull-out performance with a free-standing characteristic and 0.085 mm of thickness. Then both carbon nanomaterials free-standing papers at this stage of the study were thermally treated (TT). After the thermal treatment, significant variation was not observed in the GO paper thickness, unlike for the hybrid paper, in which the thickness was reduced from 0.085 mm to 0.073 mm. Figure 4a and 4b show the free-standing pure GO paper's SEM images. The ordered macroscopic structures of GO flake and well-defined edges without visible damage and impurities can be observed in all the samples. The average lateral size of the GO reported by the supplier is about 7.5  $\mu\text{m}$ , the same order of size observed for objects in the SEM images. These results suggest that the sonication and filtration parameters worked adequately, maintaining the expected dimensional aspect for the GO sheets at the carbon paper-like sample. Figure 3c and 3d show SEM images of the free-standing GO paper after the thermal annealing

process, where it can be observed the presence of elevated GO flakes (highlighted in the figure by red arrows) is caused by the thermal treatment. The literature<sup>33</sup> suggests that the thermal decomposition reaction of the oxygenated groups on the GO surface produces gas molecules of CO, CO<sub>2</sub>, and O<sub>2</sub>, which escape during the thermal process and disrupt the stacked structure of the paper-like film forming the gas voids paths. That can be a potential mechanism to increase the surface area of the films. This characteristic is helpful for applications such as electrodes used for supercapacitors<sup>34</sup> and nanofiltration membranes<sup>35</sup>.

Figure 5 shows SEM images of the hybrid film morphologies, untreated and treated thermally, produced by the GO/rGO/MWCNT mixture. The hybrid paper-like presents a good network constitution between the objects, with ordered macroscopic structures of graphene flakes on the carbon nanotube mat. According to the supplier, the lateral size of the rGO is between 1  $\mu\text{m}$  and 5  $\mu\text{m}$ ; therefore, the small flakes on film structure can be attributed to rGO. Analogously to pure GO paper-like results, the SEM image in Figure 4c and 4d shows the orientation of the flakes also disturbed by the thermal treatments creating the void paths suggested before. Combining one-dimensional materials (carbon nanotubes) and two-dimensional materials (graphene) to design paper-like electrodes for supercapacitor application has been extensively studied in the literature<sup>23,24,31,36-38</sup>. The results found by the authors show that the synergistic effect between carbon nanomaterials is beneficial to produce electrodes with higher total electrolyte accessible surface area. Therefore, the void paths observed for the hybrid sample can potentiate this effect.

The presence of oxygen groups linked to the graphene structure is responsible for inhibiting the electronic mobility at the GO providing a dielectric characteristic material. These groups are reported in the literature as hydroxyl (-OH) and epoxide (-C-O-C-) groups attached on the basal plane and carboxylic (-COOH) groups attached at the sheet edges<sup>39</sup>. However, this electrical insulating characteristic of GO is not suitable for energy applications. Among the methods to improve the electrical conductivity of this carbon nanomaterial, reduction by thermal annealing is widely used because it is a clean and efficient approach. The removal of the oxygen-containing groups promotes a thermal reduction of GO and consequently improves its electrical conductivity<sup>33</sup>. In this work, the TGA was used to evaluate the presence and quantify (chemical composition) of these groups in the paper-like. The correlation of thermal events observed in TGA can support comprehension of the degree of thermal reduction of the samples. Figure 6 shows the thermogravimetric (TGA), and differential thermogravimetric (DTG) curves obtained and Table 1 summarizes the main thermal events verified for the pure GO and hybrid papers-like produced. The first and second thermal events are related to the evaporation of water (and/or volatiles substances from the precursor GO or film manufacturing process) and the decomposition of functional oxygen groups, respectively. As expected, the samples treated thermally showed lower water contents (GO: 12% to 2.33%; hybrid: 6.5% to 0.6%). The smaller hygroscopic character may be related to the smaller oxygenated groups' content, which is confirmed by the second thermal event

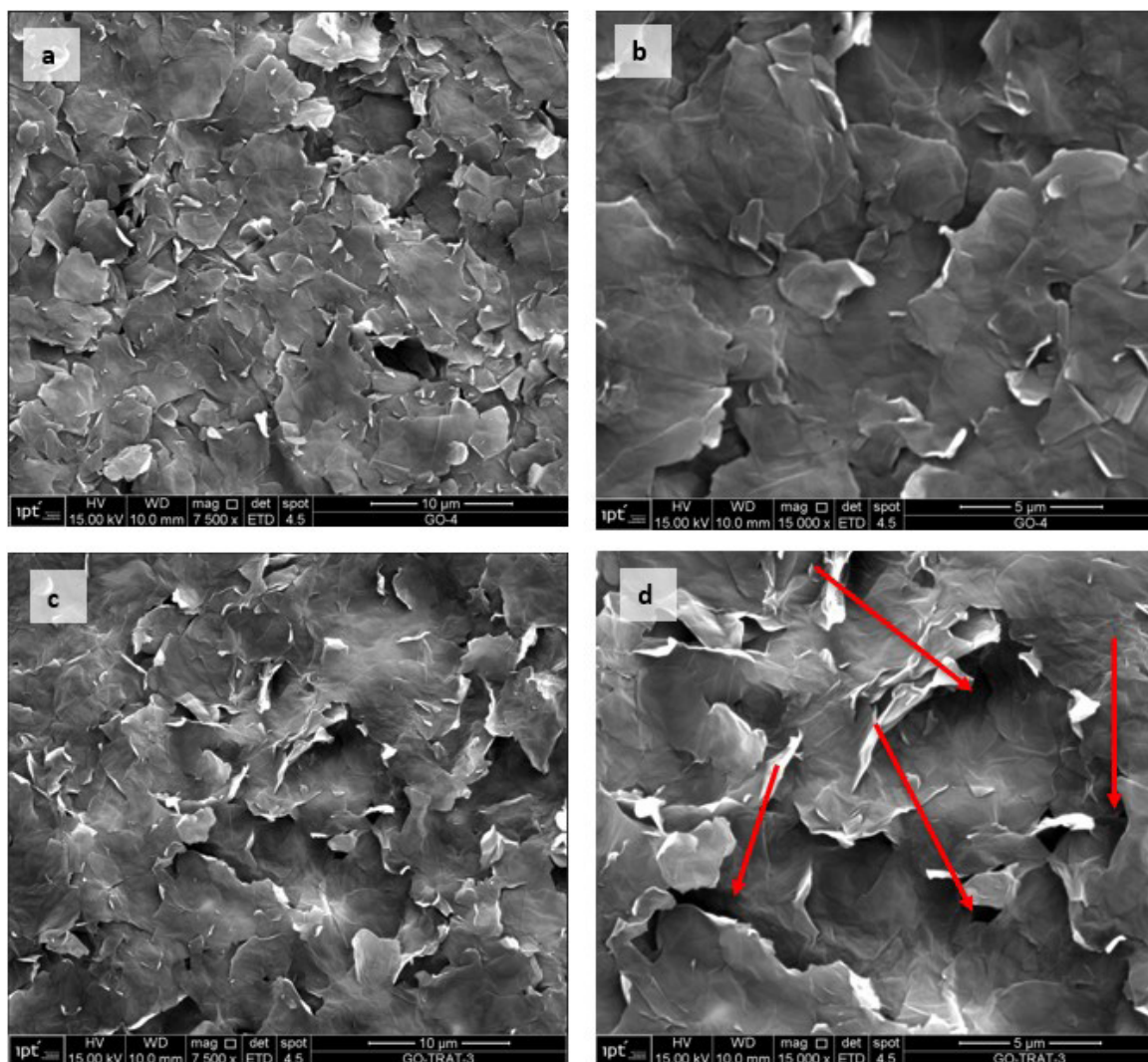


**Figure 4.** Pure GO paper-like SEM images untreated (a-b) and treated (c-d) thermally. Red arrows in (d) indicate gas voids regions caused by thermal annealing.

observed. Comparing the untreated and treated thermally samples results, the effectivity of the thermal reduction process performed in this work is confirmed by the decrease in weight loss from 27.7% to 0% (not detected) and 16.7% to 1.5% in the second thermal event observed for GO and hybrid paper-likes, respectively (Table 2). These results suggest a possible increase in the electrical conductivity of the films with the removal of the oxygen-containing groups.

Raman spectroscopy was also used to evaluate the sample crystallite size, chemical composition and thermal reduction effects. Regarding that, the Raman spectra were fitted using a combination of five functions assigned to D\*, D, D', G and D' bands (Figure 7) in the range of 1000  $\text{cm}^{-1}$  to 2000  $\text{cm}^{-1}$  and four functions assigned to G\*, 2D, D+D' and 2D' bands (Figure 8) in the range of 2000  $\text{cm}^{-1}$  to 3500  $\text{cm}^{-1}$  according to the protocol developed by Lopez-Diaz and collaborators, and Claramunt and collaborators<sup>40,41</sup>. From the data obtained from the adjustments, it was possible to calculate the ratio

of intensities of the D and G bands ( $I_D/I_G$ ), the crystallite size ( $L_A$ ) and  $Csp^2$  percentage, and the results are reported in Table 3. The  $Csp^2$  percentage was calculated in two ways proposed by Lopez-Diaz and collaborators<sup>40</sup>: from the region of the D and G bands (protocol D and G bands) and from the region of the 2D band (protocol 2D band) (Table 3). Higher  $L_A$  and  $Csp^2$  values (all protocols) and the lower  $I_D/I_G$  value are observed for all papers-like subjected to thermal treatment. These results indicate lower degree defects and the restoration of the carbon  $sp^2$  network caused by thermal annealing in the carbon nanomaterial structure present in paper-likes. Thereby, the Raman results corroborate the TGA results. Moreover, it is possible to observe the higher  $L_A$  and  $Csp^2$  values for the GO-TT [ $L_A = 7.3$ ;  $Csp^2 = 70$  (DG); 69 (2D); 61(D+D')] compared to the hybrid-TT [ $L_A = 7.1$ ;  $Csp^2 = 66$  (DG); 62 (2D); 59 (D+D')]. In this case, the restoration of the carbon  $sp^2$  network was less effective for the hybrid-TT paper-like corroborating the TGA results that

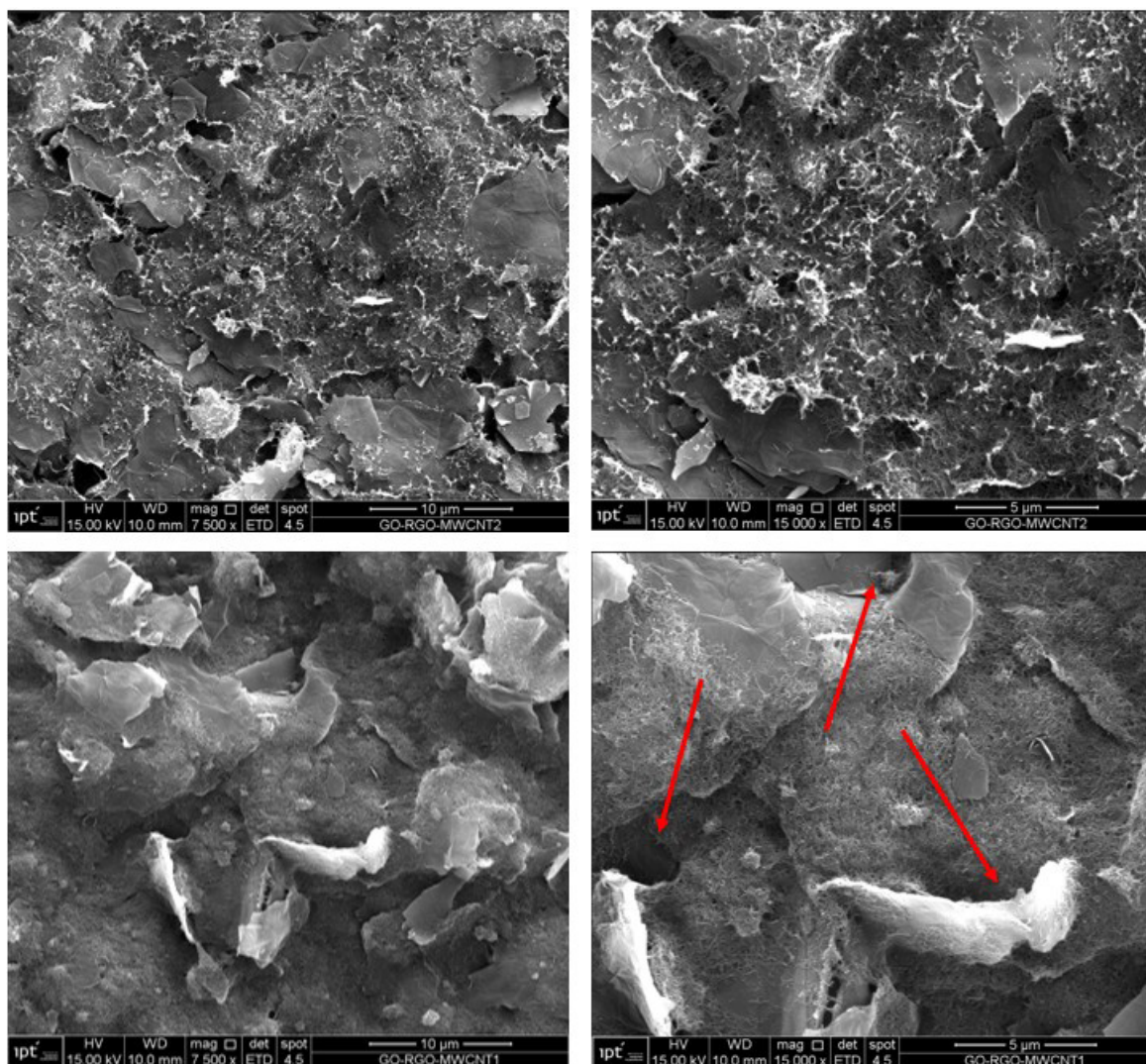


**Figure 5.** Hybrid paper-like SEM images untreated (a-b) and treated (c-d) thermally. Red arrows in (d) indicate gas voids regions caused by thermal annealing.

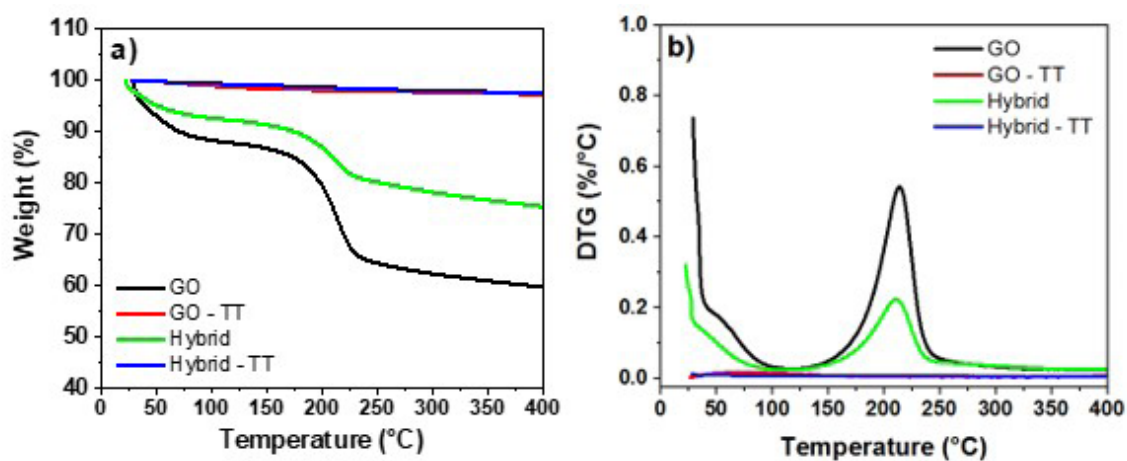


**Figure 6.** TGA (a) and DTG (b) curves of the pure GO and hybrid paper-likes untreated and treated thermally (TT) obtained at  $10\text{ }^{\circ}\text{C min}^{-1}$  in a nitrogen atmosphere.

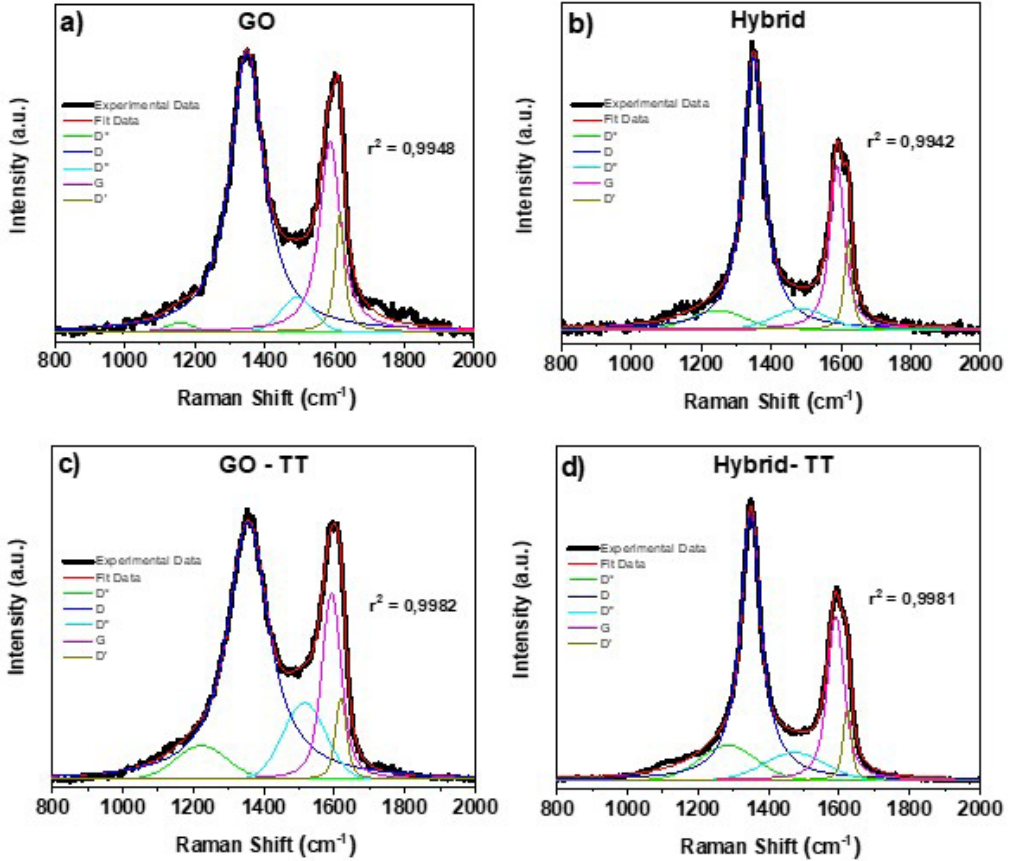
**Table 2.** Main thermal events with the maximum decomposition temperature (°C) and mass loss (%) values detected at the DTG curve for the samples.

Sample	1st	2nd
<b>GO</b>	55 °C (12.0%)	214 °C (27.7%) Onset: 173 °C / Endset: 239 °C
<b>GO - TT</b>	69 °C (2.33%)	ND*
<b>Hybrid</b>	41 °C (6.5%)	210 °C (16.7%) Onset: 160 °C / Endset: 234 °C
<b>Hybrid - TT</b>	57 °C (0.6%)	205 °C (1.5%) Onset: 160 °C / Endset: 287 °C

\*Not detected by TGA.

**Table 3.**  $I_{D'}/I_G$  value and the maximum positions of the 2D and D + D' used as parameters for estimating the  $C_{sp^2}$  percentages of paper-like samples untreated and treated according to the protocol available in the literature<sup>40,41</sup>.

Samples	Protocol D and G Bands			Protocol 2D Band			
	$I_{D'}/I_G$	$L_A$ (nm)	$C_{sp^2}$ (%)	2D Position ( $cm^{-1}$ )	$C_{sp^2}$ (%) (2D)	D+D' Position ( $cm^{-1}$ )	$C_{sp^2}$ (%) (D+D')
<b>GO</b>	1.5	6.7	59	2694	64	2934	57
<b>GO - TT</b>	1.4	7.3	70	2699	69	2936	61
<b>Hybrid</b>	1.7	6.0	41	2691	60	2691	53
<b>Hybrid - TT</b>	1.4	7.1	66	2693	62	2693	59


**Figure 7.** Raman spectra in the range of 800  $cm^{-1}$  to 2000  $cm^{-1}$  (D and G bands region) of the pure GO and hybrid paper-likes untreated (a-b) and treated thermally (TT) (c-d). The five functions (D\*, D, D'', G, and D' bands) were adjusted for all the samples according to the protocol available in the literature<sup>40,41</sup>.

showed 1.5% (Table 2) of the content of the oxygenated group still present in the hybrid sample.

Finally, considering the four-probes electrical resistance results, the papers electrical conductivities were calculated

according to the equation I, considering the respective thickness for each sample manufactured, to confirm the effect of thermal treatment of the carbon-based paper-like films. Figure 9 shows the results obtained.

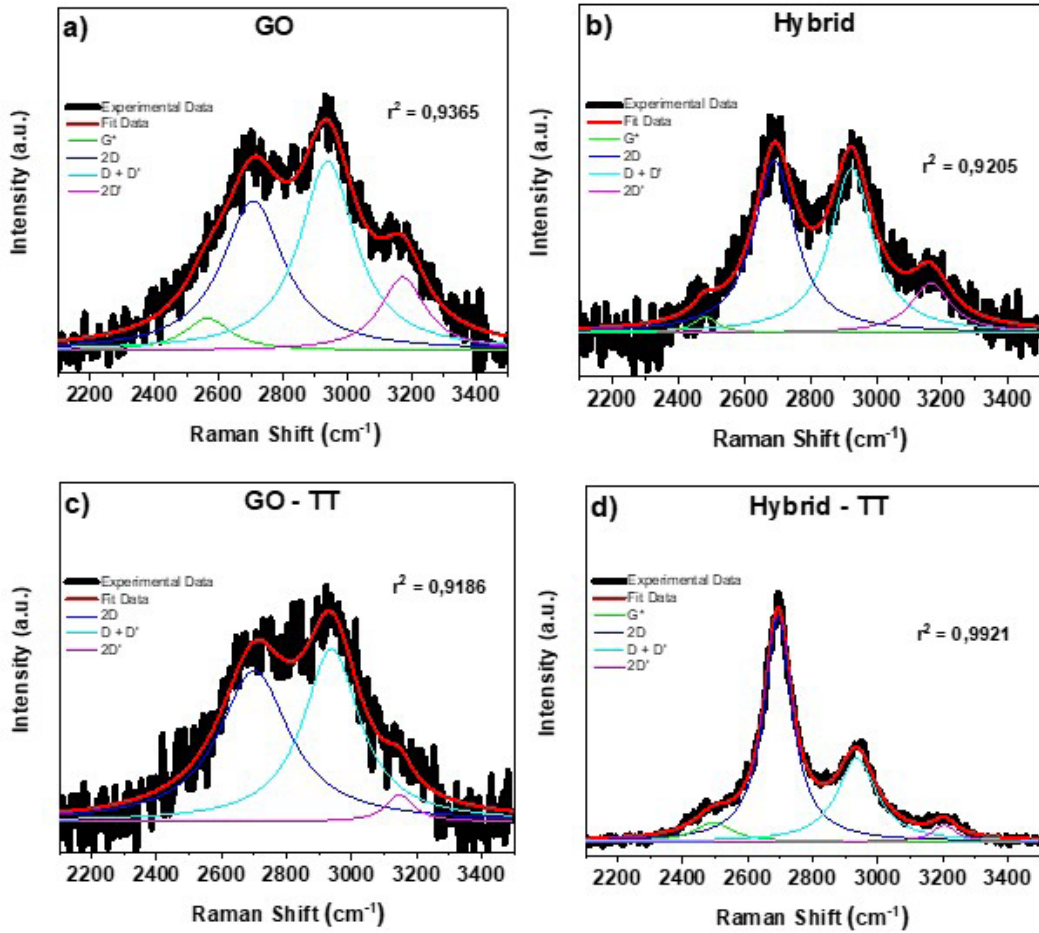


**Figure 8.** Raman spectra in the range of 2100 cm<sup>-1</sup> to 3500 cm<sup>-1</sup> (2D band region) of the pure GO and hybrid paper-likes untreated (a-b) and treated thermally (TT) (c-d). The four functions (G\*, 2D, D+D' and 2D' bands) were adjusted for all the samples according to the protocol available in the literature<sup>40,41</sup>.

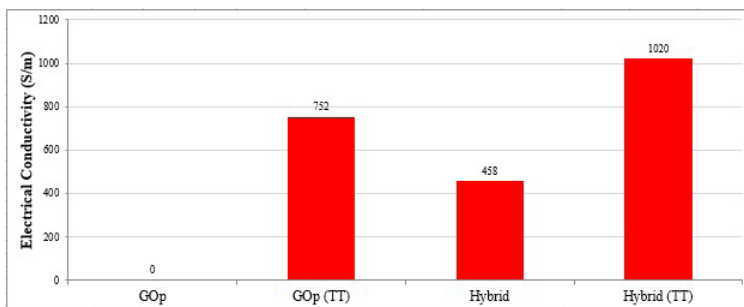


**Figure 9.** Electrical conductivity of the pure GO and hybrid paper-likes untreated and treated thermally (TT).

As expected, the pure GO paper-like untreated thermally presents an electric insulator property with a high level of resistance reported by the four-probe evaluation, supporting the previous discussions considering the presence of the oxygen groups. The hybrid paper-like untreated thermally exhibited electrical conductivity around 460 S/m. The presence of this electrical conductivity can occur by the action of the

MWCNT and the rGO attached to the GO flakes in an rGO/MWCNT networks (mat) across the film observed in the SEM images (Figures 5a and 5b). As expected, the thermally treated samples significantly improved the electrical paper properties. Considering the initial insulator characteristic of the GO papers-like, the resistivity measurement after the annealing process results in an electrical conductivity

**Table 4.** Comparison of the electrical conductivity results obtained for the graphene paper-likes in the literature with this work

Paper-Like	Ratio (wt %)	Electrical Conductivity (S/m)	Refs.
rGO	100	500	42
rGO	100	810	27
rGO	100	30000	33
rGO/MWCNT	80/20	1820	36
rGO/SWCNT	50/50	360	24
GNP/MWCNT	84/16	11.5	23
MWCNT	100	1000	29
rGO/ MWCNT	85/15	2000	31
GO	100	0	<b>Present Work</b>
GO - TT	100	752	
Hybrid (GO/rGO/ MWCNT)	25/25/50	458	
Hybrid (rGO/ MWCNT) – TT	25/25/50	1020	

film of around 750 S/m. The resistivity measurement at the hybrid paper-like shows an increase of 45%, resulting in an electric conductivity film of 1020 S/m. The increased electrical conductivity observed confirms that the thermal annealing affords the thermal reduction and restoration of the carbon  $sp^2$  network of the graphene oxide and thus corroborating the Raman and TGA results. Furthermore, these results also indicate that the formation of gas voids by the thermal treatment observed in the SEM results seems not to be harmful to the electrical conductivity of the paper-like. Table 4 presents an electrical conductivity comparison between some literature graphene paper-like references and the free-standing papers produced in the present work. It is important to note that the manufacturing process, treatment, and paper thickness can be different between the reported materials, therefore influencing the electrical conductivity results directly.

#### 4. Conclusion

During the experiments performed in this work, it was possible to understand the necessity of GO presence to obtain a free-standing paper that allows manipulation without damaging the film's integrity. Additionally, it was also observed that a pure GO paper-like presents a higher flexible structure than the hybrid paper-like before and after the thermal treatment. The SEM results showed ordered macroscopic structures of the paper-likes obtained, with GO flakes and well-defined edges without visible damage and impurities. Considering the carbon nanomaterials papers morphologies observed, it is suggested that releasing oxygenated groups from GO contributes to path formations in the paper. This effect can be a potential mechanism to improve the active surface area, known as important propriety for different applications as an electrode and nanofiltration membrane. The TGA and Raman results showed the thermal reduction and the restoration of the carbon  $sp^2$  network of the graphene oxide induced by thermal treatment. Due to

this effect, an increase in electrical conductivity to the pure GO paper-like was reported after the annealing processes achieved 752 S/m, and a 45% improvement for the hybrid treated paper-like, representing 1020 S/m. Regarding the manufacturing methods applied, the authors consider these electrical conductivity results reasonable, and a paper thickness reduction is a potential easy route to improve the performances obtained, as well as expected by working at the thermal treatment parameters. Finally, this work confirms that the vacuum filtration manufacturing process followed by a mild thermal annealing process (400°C) seems to be an efficient way to obtain free-standing and electrical conductivity carbon nanomaterials papers.

#### 5. Acknowledgements

The authors would like kindly to thanks the infrastructure availabilities provided by the *Instituto de Pesquisas Tecnológicas do Estado de São Paulo (IPT)*, the Materials and Technology Department of the School of Engineering from *Universidade Estadual Paulista (UNESP)* at Guaratinguetá Campus and the *Laboratório de Plasmas e Processos (LPP)* from *Instituto Tecnológico de Aeronáutica do Brasil*. The LPP gently provided the analysis on the four-point test fixture equipment. The authors would specially thank the contribution of the researcher, Fabiano dos Santos from the *Laboratório de Corrosão e Proteção (LCP)* from IPT by the MEV contribution. The authors also would thank the financial support received from the *Fundação de Apoio ao Instituto de Pesquisas Tecnológicas (FIPT)*. Also, the authors are grateful the financial support given by National Council for Scientific and Technological Development (CNPq) (306576/2020-1 and 304876/2020-8) and this study was financed in part by the Coordenação de Aperfeiçoamento de Pessoal de Nível Superior – Brasil (CAPES) – Finance Code 001.

#### 6. References

- Novoselov KS, Geim AK, Morozov SV, Jiang D, Zhang Y, Dubonos SV, et al. DISCOVER of Graphene: electric field effect in atomically thin carbon films. *Science*. 2004;306(5696):666-9.
- Kong W, Kum H, Bae SH, Shim J, Kim H, Kong L, et al. Path towards graphene commercialization from lab to market. *Nat Nanotechnol*. 2019;14(10):927-38. <http://dx.doi.org/10.1038/s41565-019-0555-2>.
- Reiss T, Hjelt K, Ferrari AC. Graphene is on track to deliver on its promises. *Nat Nanotechnol*. 2019;14(10):907-10. <http://dx.doi.org/10.1038/s41565-019-0557-0>.
- Novoselov KS, Fal'ko V, Colombo L, Gellert PR, Schwab MG, Kim K. A roadmap for graphene. *Nature*. 2012;490:192-200. <http://dx.doi.org/10.1038/nature11458>.
- Javaid A, Ho KKC, Bismarck A, Steinke JHG, Shaffer MSP, Greenhalgh ES. Carbon fibre-reinforced poly(ethylene glycol) diglycidylether based multifunctional structural supercapacitor composites for electrical energy storage applications. *J Compos Mater*. 2016;50(16):2155-63. <http://dx.doi.org/10.1177/0021998315602324>.
- Dimov D, Amit I, Gorrie O, Barnes MD, Townsend NJ, Neves AIS, et al. Ultrahigh performance nanoengineered graphene-concrete composites for multifunctional applications. *Adv Funct Mater*. 2018;28(23):1705183. <http://dx.doi.org/10.1002/adfm.201705183>.
- Karim N, Sarker F, Afroj S, Zhang M, Potluri P, Novoselov KS. Sustainable and multifunctional composites of graphene-based

- natural jute fibers. *Adv Sustain Syst.* 2021;5(3):2000228 <http://dx.doi.org/10.1002/adsu.202000228>.
8. Maji S, Paul AD, Das P, Chatterjee S, Chatterjee P, Dhanak VR, et al. Improved resistive switching performance of graphene oxide-based flexible ReRAM with HfOx buffer layer. *J Mater Sci Mater Electron.* 2021;32(3):2936-45. <http://dx.doi.org/10.1007/s10854-020-05045-4>.
  9. Ranjan P, Tiwary P, Chakraborty AK, Mahapatra R, Thakur AD. Graphene oxide based free-standing films for humidity and hydrogen peroxide sensing. *J Mater Sci Mater Electron.* 2018;29(18):15946-56. <http://dx.doi.org/10.1007/s10854-018-9680-1>.
  10. Tiwary P, Chatterjee SG, Singha SS, Mahapatra R, Chakraborty AK. Room temperature ethanol sensing by chemically reduced graphene oxide film. *FlatChem.* 2021;30:100317. <http://dx.doi.org/10.1016/j.flatc.2021.100317>.
  11. Miao P, Wang J, Zhang C, Sun M, Cheng S, Liu H. Graphene nanostructure-based tactile sensors for electronic skin applications. *Nanomicro Lett.* 2019;11(1):71. <http://dx.doi.org/10.1007/s40820-019-0302-0>.
  12. Chen L, Li Y, Chen L, Li N, Dong C, Chen Q, et al. A large-area free-standing graphene oxide multilayer membrane with high stability for nanofiltration applications. *Chem Eng J.* 2018;345:536-44. <http://dx.doi.org/10.1016/j.cej.2018.03.136>.
  13. Abraham J, Vasu KS, Williams CD, Gopinadhan K, Su Y, Cherian CT, et al. Tunable sieving of ions using graphene oxide membranes. *Nat Nanotechnol.* 2017;12(6):546-50. <http://dx.doi.org/10.1038/nnano.2017.21>.
  14. Agresti A, Pescetelli S, Palma AL, Del Rio Castillo AE, Konios D, Kakavelakis G, et al. Graphene Interface Engineering for Perovskite Solar Modules: 12.6% Power Conversion Efficiency over 50 cm<sup>2</sup> Active Area. *ACS Energy Lett.* 2017;2(1):279-87. <http://dx.doi.org/10.1021/acsenenergylett.6b00672>.
  15. Agrawalla RK, Paul S, Sahoo PK, Chakraborty AK, Mitra AK. A facile synthesis of a novel three-phase nanocomposite: single-wall carbon nanotube/silver nanohybrid fibers embedded in sulfonated polyaniline. *J Appl Polym Sci.* 2015. <http://dx.doi.org/10.1002/app.41692>.
  16. Chakrabarty N, Chakraborty AK, Kumar H. Nickel-hydroxide-nanohexagon-based high-performance electrodes for supercapacitors: a systematic investigation on the influence of six different carbon nanostructures. *J Phys Chem C.* 2019;123(48):29104-15. <http://dx.doi.org/10.1021/acs.jpcc.9b07234>.
  17. Baptista JM, Sagu JS, Kg UW, Lobato K. State-of-the-art materials for high power and high energy supercapacitors: performance metrics and obstacles for the transition from lab to industrial scale – A critical approach. *Chem Eng J.* 2019;374:1153-79. <http://dx.doi.org/10.1016/j.cej.2019.05.207>.
  18. Manoharan S, Krishnamoorthy K, Sathyaseelan A, Kim SJ. High-power graphene supercapacitors for the effective storage of regenerative energy during the braking and deceleration process in electric vehicles. *Mater Chem Front.* 2021;5(16):6200-11. <http://dx.doi.org/10.1039/D1QM00465D>.
  19. Wong SI, Sunarso J, Wong BT, Lin H, Yu A, Jia B. Towards enhanced energy density of graphene-based supercapacitors: current status, approaches, and future directions. *Journal of Power Sources.* 2018;396:182-206. <https://doi.org/10.1016/j.jpowsour.2018.06.004>.
  20. Ngo C, Fitzgerald MA, Dzara MJ, Strand MB, Diercks DR, Pylypenko S. 3D atomic understanding of functionalized carbon nanostructures for energy applications. *ACS Appl Nano Mater.* 2020;3(2):1600-11. <http://dx.doi.org/10.1021/acsnm.9b02360>.
  21. Oishi SS, Rezende MC, Origo FD, Damião AJ, Botelho EC. Viscosity, pH, and moisture effect in the porosity of poly(furfuryl alcohol). *J Appl Polym Sci.* 2013. <http://dx.doi.org/10.1002/app.38332>.
  22. Gaefke CB, Botelho EC, Ferreira NG, Rezende MC. Effect of furfuryl alcohol addition on the cure of furfuryl alcohol resin used in the glassy carbon manufacture. *J Appl Polym Sci.* 2007;106(4):2274-81. <http://dx.doi.org/10.1002/app.26938>.
  23. Lu X, Dou H, Gao B, Yuan C, Yang S, Hao L, et al. A flexible graphene/multiwalled carbon nanotube film as a high performance electrode material for supercapacitors. *Electrochim Acta.* 2011;56(14):5115-21. <http://dx.doi.org/10.1016/j.electacta.2011.03.066>.
  24. Jha N, Ramesh P, Bekyarova E, Itkis ME, Haddon RC. High energy density supercapacitor based on a hybrid carbon nanotube-reduced graphite oxide architecture. *Adv Energy Mater.* 2012;2(4):438-44. <http://dx.doi.org/10.1002/aenm.201100697>.
  25. Jin K, Zhang W, Wang Y, Guo X, Chen Z, Li L, et al. In-situ hybridization of polyaniline nanofibers on functionalized reduced graphene oxide films for high-performance supercapacitor. *Electrochim Acta.* 2018;285:221-9. <http://dx.doi.org/10.1016/j.electacta.2018.07.220>.
  26. Cheng Q, Tang J, Shinya N, Qin LC. Co(OH)<sub>2</sub> nanosheet-decorated graphene-CNT composite for supercapacitors of high energy density. *Sci Technol Adv Mater.* 2014;15(1):014206. <http://dx.doi.org/10.1088/1468-6996/15/1/014206>.
  27. Vallés C, David Núñez J, Benito AM, Maser WK. Flexible conductive graphene paper obtained by direct and gentle annealing of graphene oxide paper. *Carbon.* 2012;50(3):835-44. <http://dx.doi.org/10.1016/j.carbon.2011.09.042>.
  28. Nanografi Nano Technology. Commercial Website. 2022 [cited 2022 Mar 17]. Available from: <https://nanografi.com/>
  29. Ribeiro B, Corredor JAR, de Paula Santos LF, Gomes NAS, Rezende MC. Electrical conductivity and electromagnetic shielding performance of glass fiber-reinforced epoxy composites with multiwalled carbon nanotube buckypaper interlayer. *J Mater Sci Mater Electron.* 2021;32(2):1962-76. <http://dx.doi.org/10.1007/s10854-020-04964-6>.
  30. Trigueiro JPC, Lavall RL, Silva GG. Supercapacitors based on modified graphene electrodes with poly(ionic liquid). *J Power Sources.* 2014;256:264-73. <http://dx.doi.org/10.1016/j.jpowsour.2014.01.083>.
  31. Trigueiro JPC, Lavall RL, Silva GG. Nanocomposites of graphene nanosheets/multiwalled carbon nanotubes as electrodes for in-plane supercapacitors. *Electrochim Acta.* 2016;187:312-22. <http://dx.doi.org/10.1016/j.electacta.2015.11.053>.
  32. Liu S, Hu K, Cerruti M, Barthelat F. Ultra-stiff graphene oxide paper prepared by directed-flow vacuum filtration. *Carbon.* 2020;158:426-34. <http://dx.doi.org/10.1016/j.carbon.2019.11.007>.
  33. Yang Y, Shen H, Yang J, Ren X, Gao K, Wang Z. Enhanced conductivity and flexibility in reduced graphene oxide paper by combined chemical-thermal reduction. *J Electron Mater.* 2021;50(12):6991-9. <http://dx.doi.org/10.1007/s11664-021-09201-2>.
  34. Ye X, Zhu Y, Tang Z, Wan Z, Jia C. In-situ chemical reduction produced graphene paper for flexible supercapacitors with impressive capacitive performance. *J Power Sources.* 2017;360:48-58. <http://dx.doi.org/10.1016/j.jpowsour.2017.05.103>.
  35. Liu G, Jin W, Xu N. Graphene-based membranes. *Chem Soc Rev.* 2015;44(15):5016-30. <http://dx.doi.org/10.1039/C4CS00423J>.
  36. Sun M, Wang G, Li X, Li C. Irradiation preparation of reduced graphene oxide/carbon nanotube composites for high-performance supercapacitors. *J Power Sources.* 2014;245:436-44. <http://dx.doi.org/10.1016/j.jpowsour.2013.06.145>.
  37. Bondavalli P, Delfaure C, Privat D, Legagneux P. Supercapacitor electrode based on mixtures of graphene/graphite and carbon nanotubes fabricated using a new dynamic air-brush deposition technique. *Proc. SPIE 8814, Carbon Nanotubes, Graphene, and Associated Devices VI.* 2013:88140F. <http://dx.doi.org/10.1117/12.2024973>.
  38. Yu D, Dai L. Self-assembled graphene/carbon nanotube hybrid films for supercapacitors. *J Phys Chem Lett.* 2010;1(2):467-70. <http://dx.doi.org/10.1021/jz9003137>.

39. Márquez-Lamas U, Martínez-Guerra E, Toxqui-Terán A, Aguirre-Tostado FS, Lara-Ceniceros TE, Bonilla-Cruz J. Tuning the mechanical, electrical, and optical properties of flexible and free-standing functionalized graphene oxide papers having different interlayer d spacing. *J Phys Chem C*. 2017;121(1):852-62. <http://dx.doi.org/10.1021/acs.jpcc.6b09961>.
40. López-Díaz D, López Holgado M, García-Fierro JL, Velázquez MM. Evolution of the raman spectrum with the chemical composition of graphene oxide. *J Phys Chem C*. 2017;121(37):20489-97. <http://dx.doi.org/10.1021/acs.jpcc.7b06236>.
41. Claramunt S, Varea A, López-Díaz D, Velázquez MM, Cornet A, Cirera A. The importance of interbands on the interpretation of the raman spectrum of graphene oxide. *J Phys Chem C*. 2015;119(18):10123-9. <http://dx.doi.org/10.1021/acs.jpcc.5b01590>.
42. Lin X, Shen X, Zheng Q, Yousefi N, Ye L, Mai YW, et al. Fabrication of highly-aligned, conductive, and strong graphene papers using ultralarge graphene oxide sheets. *ACS Nano*. 2012;6(12):10708-19. <http://dx.doi.org/10.1021/nn303904z>.